



# Analysis of prognostic oncogene filaggrin (*FLG*) wild-type subtype and its implications for immune checkpoint blockade therapy in bladder urothelial carcinoma

Liang Chen<sup>1</sup>, Xiaobo Huang<sup>1</sup>, Liulin Xiong<sup>1</sup>, Weinan Chen<sup>1</sup>, Lizhe An<sup>1</sup>, Huanrui Wang<sup>1</sup>, Yang Hong<sup>1</sup>, Huina Wang<sup>2</sup>

<sup>1</sup>Urology and Lithotripsy Center, Peking University People's Hospital, Beijing, China; <sup>2</sup>Acornmed Biotechnology Co., Ltd., Beijing, China

**Contributions:** (I) Conception and design: L Chen; (II) Administrative support: None; (III) Provision of study materials or patients: None; (IV) Collection and assembly of data: X Huang, L Xiong, W Chen, L An, HR Wang, Y Hong; (V) Data analysis and interpretation: X Huang, L Xiong, W Chen, HN Wang; (VI) Manuscript writing: All authors; (VII) Final approval of manuscript: All authors.

**Correspondence to:** Liang Chen. Urology and Lithotripsy Center, Peking University People's Hospital, Beijing, China. Email: DrChenliang1201@163.com.

**Background:** Bladder urothelial carcinoma (BLCA) is one of the most common urinary tract malignant tumors. Immune checkpoint blockade (ICB) therapy has significantly progressed the treatment of BLCA. This study aimed to investigate the role of specific genetic mutations that may serve as immune biomarkers for ICB therapy in BLCA.

**Methods:** Mutation information and expression profiles were acquired from The Cancer Genome Atlas (TCGA) database. Integrated bioinformatics analysis was carried out to explore the subtypes with poor prognosis of BLCA. Functional enrichment analysis was also conducted. The infiltrating immune cells and the prediction of ICB response between different subtypes were explored using the immuCellAI algorithm. Cell Counting Kit-8 (CCK-8) and flow cytometry assays were conducted to explore the effect of filaggrin (*FLG*) knockdown in BLCA 5637 and T24 cell lines.

**Results:** An overview of mutation information in BLCA patients was shown. *FLG* was identified to be strongly associated with the prognosis of BLCA patients and *FLG* wild-type was associated with poorer outcome. Prognostic *FLG* wild-type was divided into 2 subtypes (Sub1 and Sub2). Following an investigation of the subtypes, Sub2 of *FLG* wild-type was found to be associated with poorer outcome in BLCA. The differentially expressed genes (DEGs) between Sub1 and Sub2 were screened out and the DEGs were enriched in malignant tumor proliferation, DNA damage repair, and immune-related pathways. Furthermore, Sub2 of *FLG* wild-type was associated with infiltrated immune cells, and responded worse to ICB. Sub2 of *FLG* wild-type may be used as a biomarker to predict the prognosis of BLCA patients receiving ICB. The cellular experiments revealed that knockdown of *FLG* could suppress BLCA cell proliferation and promote apoptosis.

**Conclusions:** *FLG* is an oncogene that may affect the prognosis of BLCA patients through mutation. Sub2 of *FLG* wild-type is associated with poor prognosis and can be used to predict ICB response for BLCA treatment. This research provides a new basis and ideas for guiding the clinical application of BLCA immunotherapy.

**Keywords:** Bladder urothelial carcinoma (BLCA); filaggrin (*FLG*); subtype; mutations; immune checkpoint blockade (ICB)

Submitted Jul 29, 2022. Accepted for publication Oct 14, 2022.

doi: 10.21037/tau-22-573

**View this article at:** <https://dx.doi.org/10.21037/tau-22-573>

## Introduction

Bladder urothelial carcinoma (BLCA) is one of the most common urinary tract malignant tumors and accounts for nearly 170,000 deaths annually worldwide (1). It is the ninth most incident neoplasm in China and the 10th most common malignant tumor worldwide (2). BLCA has become a serious public health problem because of its high incidence, high risk of recurrence, and high frequency of treatment failure (e.g., intravesical bacillus Calmette–Guerin or platinum-based chemotherapy) (3). The treatment for BLCA has remained conservative and the curative effect has not made a breakthrough (4). Due to the large number of recognizable antigens, BLCA might be sensitive to immunotherapy (5). With the rapid development of immunotherapy, immune checkpoint blockade (ICB) has become a novel treatment strategy for BLCA (6). ICB refers to inhibitory drugs developed for immune checkpoints, which can rejuvenate immune cells and kill tumor cells again (7). Therefore, the prediction of immune checkpoints is of clinical significance.

The filaggrin (*FLG*) gene can encode a related protein that accumulates in the intermediate filaments of mammalian epidermal keratin (8). Previous studies have shown variability in the frequency of *FLG* variants (9). The mutation of *FLG* is associated with a variety of skin diseases (10) and cancers such as head and neck cancer, prostate cancer, urinary cancer, and bronchus and lung cancer (11). It is suggested that *FLG* gene mutation is one of the risk factors for cancer, as the associations between *FLG* loss-of-function mutations and cancer have been demonstrated in subgroup analyses (11). Besides, a previous study has shown that BLCA is a highly mutated tumor type (12). However, the associations between *FLG* mutation subtypes and BLCA need further investigation.

In the present study, we aimed to investigate the prognosis and immune checkpoint prediction role of *FLG* gene subtypes in BLCA. Mutation information and expression profiles were acquired from The Cancer Genome Atlas (TCGA) database. Integrated bioinformatics analysis was carried out to explore the mutation genes of BLCA and *FLG*. Following study of the subtypes of *FLG* and functional enrichment analysis, their relationships with prognosis and immune infiltration were also evaluated. Finally, we demonstrated the important role of *FLG* subtype in ICB. This research provides a new basis and ideas for guiding the clinical use of BLCA immunotherapy. We present the following article in accordance with the MDAR

reporting checklist (available at <https://tau.amegroups.com/article/view/10.21037/tau-22-573/rc>).

## Methods

### *Data source, collection, and processing*

Transcriptome data and clinical information of BLCA patients were downloaded from TCGA data portal (<http://cancergenome.nih.gov/>). The study was conducted in accordance with the Declaration of Helsinki (as revised in 2013). The “maftools” R package was used to analyze the Mutation Annotation Format (MAF) file and visualize the somatic mutation data (13).

### *Identification of gene expression-based subtypes*

Unsupervised clustering was performed using the R package “ConsensusClusterPlus” for class discovery based on the comparison of gene expression profiles (14), and 80% item resampling, 50 resamplings, and a maximum evaluated K of 10 were selected for clustering. The cumulative distribution function (CDF) and consensus heat map were used to assess the optimal K.

### *Differential expression analysis*

The differentially expressed mRNAs presented in a heat map and volcano plot were screened using the “GDCRNATools” package, with the criteria of  $|\log_2[\text{fold change (FC)}]| > 1$  and false discovery rate (FDR)  $< 0.05$ .

### *Functional enrichment analysis*

To assess the function of differential genes between subtypes in BLCA, Gene Ontology (GO) annotation analyses were performed by using the “clusterProfiler” package of R software. P value  $< 0.05$  was set as the cut-off criterion. Gene set enrichment analysis (GSEA) was conducted to examine critical pathways represented under different conditions. The ridge plot was presented using clusterProfiler.

### *Immune infiltration analysis and immunotherapy prediction*

The infiltrating immune cells and the prediction of ICB response between different subtype groups were explored using the immuCellAI algorithm. The abundance

differences of 18 immune cells were estimated, with P value <0.05 recognized as a significant difference. ICB therapy response was predicted by the model based on five anti-PD-1 or CTLA4 therapy datasets (15).

### Cell culture and gene knockdown

Bladder cancer cell lines 5637 and T24 were obtained from the American Type Culture Collection (ATCC; Manassas, VA, USA). Cells were supplemented with 10% fetal bovine serum (FBS) and 1% antibiotics (penicillin-streptomycin) and maintained at 37 °C and 5% CO<sub>2</sub>. To knockdown *FLG* expression in these 2 cell lines, transfection was performed using Lipofectamine RNAiMAX Reagent (Invitrogen, Carlsbad, CA, USA) according to the manufacturer's instructions. The cells in Transwell™-Clear well inserts were transfected with the respective siRNAs for 24 h before culturing for 7 days. The siRNAs for *FLG* were as follows:

- ❖ SiRNA1: sense, 5'-GCACAGUCAUCAUGAUAAACA-3'; antisense, 5'-UUUAUCAUGAUGACUGUGCUU-3';
- ❖ SiRNA2: sense, 5'-GGAUAUUCACCUACUCAUAGA-3'; antisense, 5'-UAUGAGUAGGUGAAUAUCCUU-3';
- ❖ SiRNA3: sense, 5'-AGAAGUGCAAGCAGACAAACA-3'; antisense, 5'-UUUAUCAUGAUGACUGUGCUU-3'.

### RNA isolation and quantitative real-time polymerase chain reaction (qRT-PCR)

Total RNA was extracted from bladder cancer cell lines 5637 and T24 using the TRIzol reagent (Invitrogen, Carlsbad, CA, USA). For first-strand cDNA synthesis, 1 µg of total RNA was reverse-transcribed in a 20 µL reaction using the PrimeScript RT Reagent kit (Takara Bio, Kusatsu, Japan). The cDNA samples were amplified in triplicate via qRT-PCR using the MxPro-Mx3005P Real Time PCR system (Agilent Technologies, Santa Clara, CA, USA) and SYBR Premix ExTaq (Takara Bio) according to the manufacturer's instructions. The qRT-PCR cycling conditions were as follows: initial denaturation at 95 °C for 1 min, 95 °C for 35 s, and annealing at 60 °C for 35 s for 40 cycles. The 2<sup>-ΔΔCT</sup> method, with *GAPDH* as the internal control, was used to determine relative mRNA expression. The fluorescent signals were measured after each primer-annealing step at 60 °C. The primer sequences for *FLG* and *GAPDH* were as follows:

- ❖ *FLG*: forward, 5'-TGAAGCCTATGACACCAC TGA-3'; reverse, 5'-TCCCCTACGCTTTCTTG TCCT-3';
- ❖ *GAPDH*: forward, 5'-GGAGCGAGATCCCTCC AAAAT-3'; reverse, 5'-GGCTGTTGTCATACTTC TCATGG-3'.

### Cell Counting Kit-8 (CCK-8) assay

Cell proliferation was measured using CCK-8 (DojinDO, Japan) assays every 24 h for 3 days. Transfected cells (1×10<sup>4</sup> cells/well) were seeded into 96-well plates and cultured at 37 °C with 5% CO<sub>2</sub>. After incubation with CCK-8 solution (10 µL) for 2 h, the absorbance was measured at 450 nm using a spectrophotometer (Thermo Fisher, USA).

### Flow cytometric assay

Cell apoptosis was assessed using the Annexin V-fluorescein isothiocyanate (FITC)/propidium iodide (PI) apoptosis detection kit (BD Biosciences, USA) according to the manufacturer's instructions. In brief, 5637 and T24 cells were collected and washed with phosphate-buffered saline (PBS) after relevant treatment and transfection. Then, cells were suspended in 500 µL binding buffer, and 5 µL Annexin V-FITC and 5 µL PI were applied to stain cells at room temperature in the dark for 15 min. Finally, the cell apoptotic rate was analyzed by a FACScan® flow cytometer (BD Biosciences) and determined using FlowJo software (7.6.1; FlowJo LLC).

### Statistical analysis

All bioinformatic analyses were operated on R software. All statistical analyses for biological experiments were conducted with GraphPad 8.0. All experiments were performed at least 3 times. Means ± standard deviations (SD) were used to express quantitative data. One-way analysis of variance (ANOVA) was applied to compare differences between the 2 groups. A value of P<0.05 indicated that the difference was statistically significant.

## Results

### Genetic mutation profiles in BLCA

The evolution of bladder cancer is strongly correlated with mutational events at the genome level, including multiple

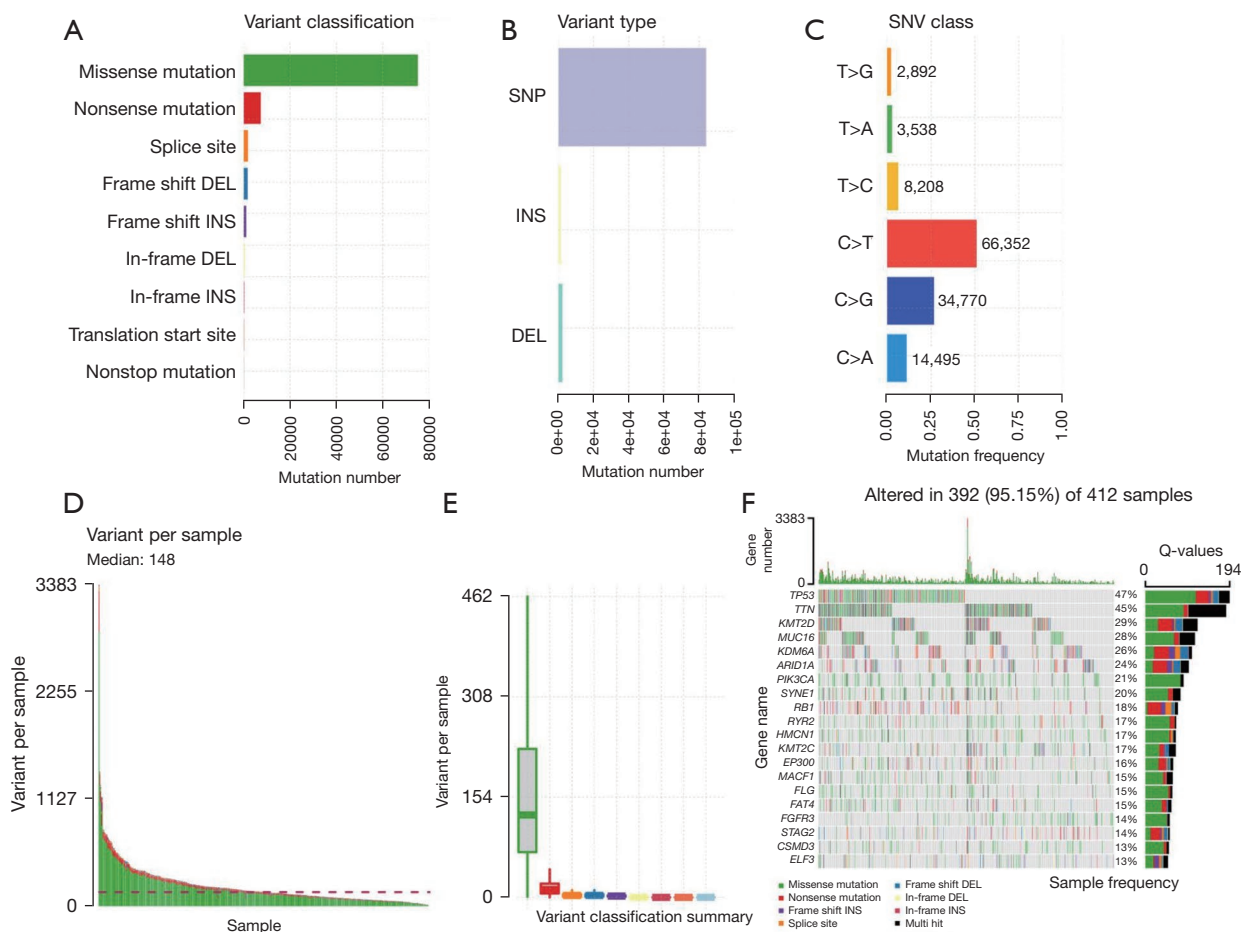


**Figure 1** Overview of mutation information in BLCA patients. (A-C) Variant classifications (A), variant types (B), and SNV classes (C) in BLCA samples. (D) Variants per samples. (E) Variant classification summary. (F) Waterfall plot showing the mutation information for the top 20 genes. Side bar plot shows log<sub>10</sub> transformed Q-values estimated by MutSigCV. BLCA, bladder urothelial carcinoma; SNP, single nucleotide polymorphism; INS, insertion; DEL, deletion; SNV, single nucleotide variants.

tumor suppressors and oncogenes (16). To systematically analyze the genetic mutational landscape in BLCA, somatic genetic mutation data from TCGA database was downloaded for subsequent analysis. First, missense mutations accounted for the majority of all variant mutations (Figure 1A). Specifically, single nucleotide polymorphisms (SNPs) represented the largest fraction in variant type compared with insertions or deletions (Figure 1B). The most common single nucleotide variant (SNV) was C>T, followed by C>G and C>A (Figure 1C). The median of per variants samples was 148 (Figure 1D) and the variants classification summary is shown in Figure 1E.

We also demonstrated the top 20 hotspot mutated genes and their mutation frequencies in Figure 1F. Consistent with

other cell types, the well-known tumor suppressor gene *TP53* ranked the highest, with a mutation frequency of 47%. Titin (*TTN*) ranked second, with a mutation frequency of 45%. The mutation status of *TTN* has been linked with chemotherapy and ICB response in lung cancer and other cell types (17,18). Notably, 5 histone modifiers showed higher mutation frequencies, such as *KMT2D* (29%), *KDM6A* (26%), *ARID1A* (24%), and *KMT2C* (17%), suggesting a genetic mutation-epigenetic disturbance in bladder cancer progression. Other hotspot mutation genes included *MUC16* (28%), *PIK3CA* (21%), *SYNE1* (20%), and *RB1* (18%). Other relative lower frequently mutated genes included *RYR2* (17%), *HMCN1* (17%), *EP300* (16%), *MACF1* (15%), *FLG* (15%), *FAT4* (15%), *FGFR3* (14%), *STAG2* (14%), and *ELF3* (13%).

### ***FLG wild-type tumors can be divided into 2 different prognostic groups***

To further analyze the impact of hotspot gene mutation on survival status, we conducted a prognostic analysis of the above top 19 mutant genes based on gene mutation status (wild-type *vs.* mutation groups) (Figure S1). As a result, *FLG* was found to be strongly related to the prognosis of patients. Notably, the survival time of *FLG* wild-type patients was significantly shorter than that of *FLG* mutant patients (Figure 2A), suggesting a tumor-promoting role of *FLG* in BLCA. Consistent with the overall mutation types, the main mutation forms of the *FLG* gene were missense mutations (Figure 2B). The mutation forms of the other top 19 mutant genes are shown in Figure S2. Based on the above results, it was clear that the research objects in BLCA were *FLG* wild-type samples. Next, we combined the transcriptome data in TCGA database to explore whether *FLG* wild-type patients with high mortality rates have different subtypes. ConsensusClusterPlus software was applied and *FLG* wild-type patients were found to be divided into 2 categories, namely Sub1 and Sub2 (Figure 2C). Then, we compared the survival status of Sub1 and Sub2, and the results showed that the survival time of Sub2 patients was significantly less than that of Sub1 patients (Figure 2D). At the same time, it could be seen that the mortality rate of Sub2 was as high as 90% (Figure 2E). The death rate of Sub1 was 46%, while the death rate of Sub2 was 90%. Overall, we found that there are 2 types of *FLG* wild-type patients, and Sub2 of *FLG* wild-type in BLCA is associated with poorer outcome.

### ***The differentially expressed genes (DEGs) between the subtypes of FLG wild-type are associated with malignant tumor proliferation and DNA damage repair***

In the next step, we used transcriptome data to explore the biological signaling pathways of DEGs between the 2 different subtypes. The DEGs between Sub1 and Sub2 were analyzed ( $|\log_2FC| > 1$  and  $FDR < 0.05$ ). A total of 778 up-regulated (e.g., *GAMT*, *RTL5*, *KLHL3*, *UGT1A6*, etc.) and 972 down-regulated DEGs (e.g., *F8A1*, *KRT16*, etc.) were identified (Figure 3A,3B). The results of Kyoto Encyclopedia of Genes and Genomes (KEGG) functional enrichment analysis based on DEGs showed that tumor proliferation-related pathways such as the MAPK signaling pathway, cell cycle, apoptosis, and tumor necrosis factor  $\alpha$  (TNF- $\alpha$ ) signaling pathway were significantly enriched

(Figure 3C,3D). Furthermore, KEGG analysis in GSEA indicated that DEGs were also related to DNA damage repair, demonstrated by the enriched signaling pathways of DNA replication, nucleotide excision repair, base excision repair, and mismatch repair. Together, these results indicated that the DEGs between the subtypes of *FLG* wild-type are associated with malignant tumor proliferation and DNA damage repair.

### ***The DEGs between the subtypes of FLG wild-type are enriched in immune-related pathways***

Next, we sequentially used transcriptome data to explore the biological significance of the 2 different subtypes of patients. The DEGs between Sub1 and Sub2 underwent GO biological process (BP) functional enrichment analysis. As shown in Figure 4A, pathways such as inflammation, chemokine production, and T cell activation were significantly enriched. The BP pathway was further analyzed by the GSEA method, and the results also showed that T cells play a key role in different types of tumor microenvironments. In addition, the results suggest that the pathways related to immunity and inflammation are significantly down-regulated, and the immune response involved in T cell activation is suppressed (Figure 4B).

### ***Sub2 of FLG wild-type is associated with infiltrated immune cells and has a worse response to ICB***

Infiltrating immune cells in tumors are a hallmark of immune surveillance and a necessary part of the complex microenvironment regulating tumor progression (19). It is known that T cells play a key role in mediating the tumor immune microenvironment, and different subtypes of T cells have different divisions of labor (20). Therefore, ImmuCellAI software was used to analyze the T cell types of *FLG* wild-type patients with different subtypes. As seen in Figure 5A, the results showed that CD4<sup>+</sup> naive T cells, central memory T cells (Tcm), and natural killer T (NKT) cells were significantly down-regulated in Sub2, while T helper type 1 (Th1) cells were significantly up-regulated in Sub2. CD4<sup>+</sup> T cells can directly eliminate tumor cells through cytolysis or indirectly regulate the tumor immune microenvironment to target tumor cells (21). NKT cells are a type of T cell subgroup with specific NK cell markers in immune cells. After activation, they can directly act as anti-tumor effector cells to have a killing effect, and they can also activate other immune effector cells, such as NK

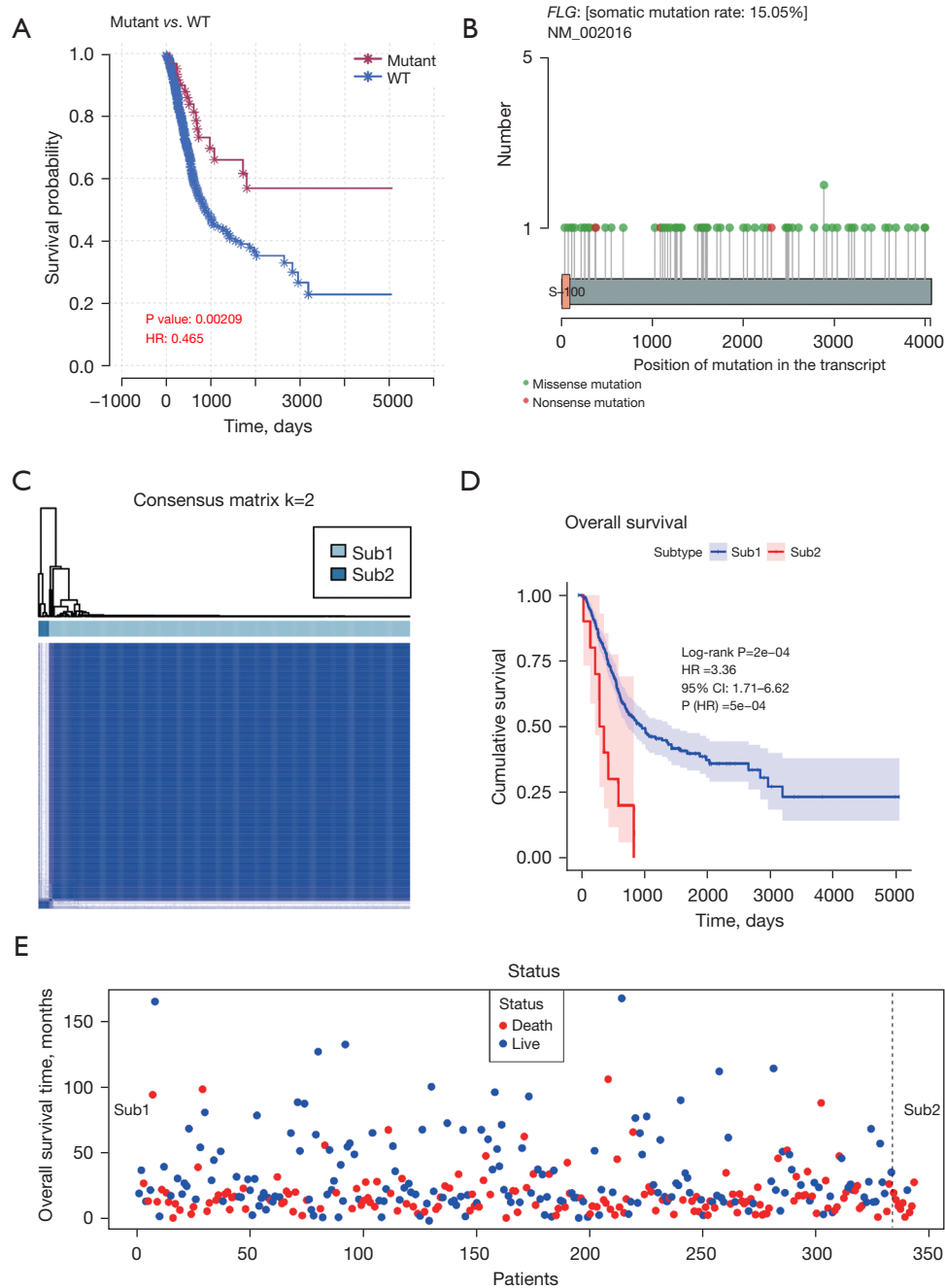


**Figure 2** Prognostic *FLG* wild-type was divided into 2 subtypes. (A) Kaplan-Meier estimates of OS of *FLG* wild-type and *FLG* mutant groups in BLCA patients. (B) *FLG* gene mutation information. (C) Identifying the subtypes of *FLG* wild-type. ConsensusClusterPlus software was used to divide the samples into 2 subtypes, namely Sub1 and Sub2. (D) Kaplan-Meier estimates of OS of Sub1 and Sub2 from *FLG* wild-type in BLCA patients. (E) Overall survival time of Sub1 and Sub2 from *FLG* wild-type in BLCA patients. WT, wild type; HR, hazard ratio; CI, confidence interval; *FLG*, filaggrin; OS, overall survival; BLCA, bladder urothelial carcinoma.

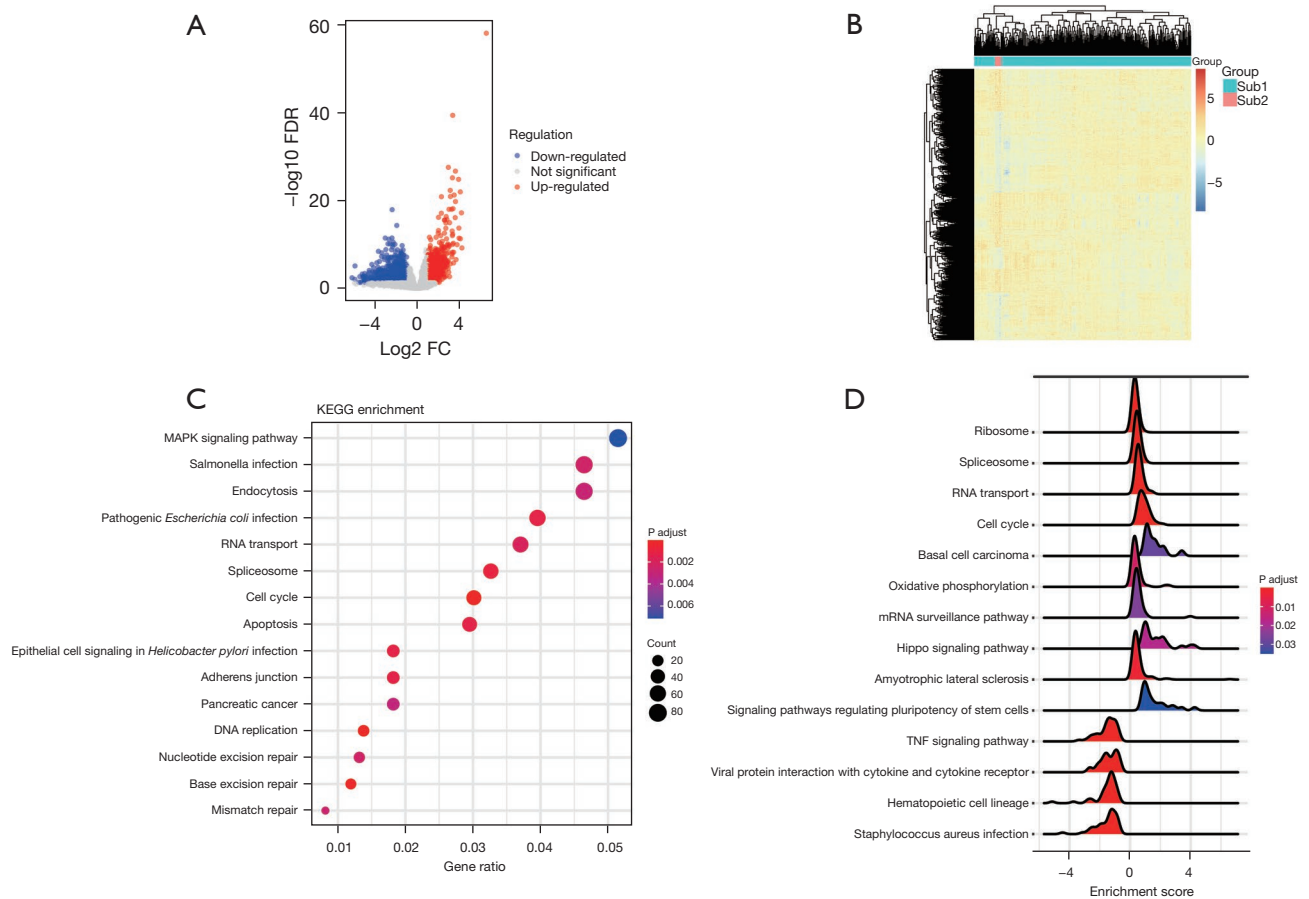


**Figure 3** The 2 subtypes of *FLG* wild-type differed in biological functions. (A,B) Volcano map (A) and heat map (B) showing DEGs between Sub1 and Sub2. (C) Bubble chart showing the top 15 enriched KEGG signaling pathways of DEGs. (D) Ridgeline plot showing the GSEA results. DEGs, differentially expressed genes; *FLG*, filaggrin; FDR, false discovery rate; FC, fold change; KEGG, Kyoto Encyclopedia of Genes and Genomes; GSEA, gene set enrichment analysis.

cells, to indirectly achieve an anti-tumor effect. NKT cells play an important role in anti-tumor immunity, acquired immune response, and immune regulation (22).

Changes in tumor microenvironment (TME), including the most influential T cells, are intensively related to the response to ICB for cancer treatment. For instance, CD4<sup>+</sup>FoxP3<sup>+</sup> Treg is recognized as the suppressor of antitumor immune response in many types of cancer (23). ICB is beneficial for restoring T lymphocyte activity and breaking through the physical barrier of the tumor immune microenvironment to promote T cell homing. Therefore, it can activate anti-tumor immunity and improve the effect of immunotherapy. Based on the results of the current study, enhanced tumor immunogenicity predicted improved clinical response to ICB. Finally, we used immuCellAI to predict the response of ICB on *FLG* wild-type patients of

different types. As shown in *Figure 5B*, the reaction rate of Sub1 was 33.7%, while the reaction rate of Sub2 was 10%. The results showed that Sub2 patients had a worse response to ICB. Altogether, the above results indicated that the detection of Sub2 *FLG* wild-type might be used in clinical immunotherapy.

### ***Knockdown of FLG suppresses BLCA cell proliferation and promotes apoptosis***

The bioinformatics analysis revealed that *FLG* plays an important role in tumor progression. Next, we performed cell experiments to verify the oncogenic role of *FLG* in BLCA cell lines 5637 and T24. Three kinds of siRNAs were used for qRT-PCR assays, and siRNA2 could significantly reduce the expression of *FLG* in both the 5637 and T24 cell

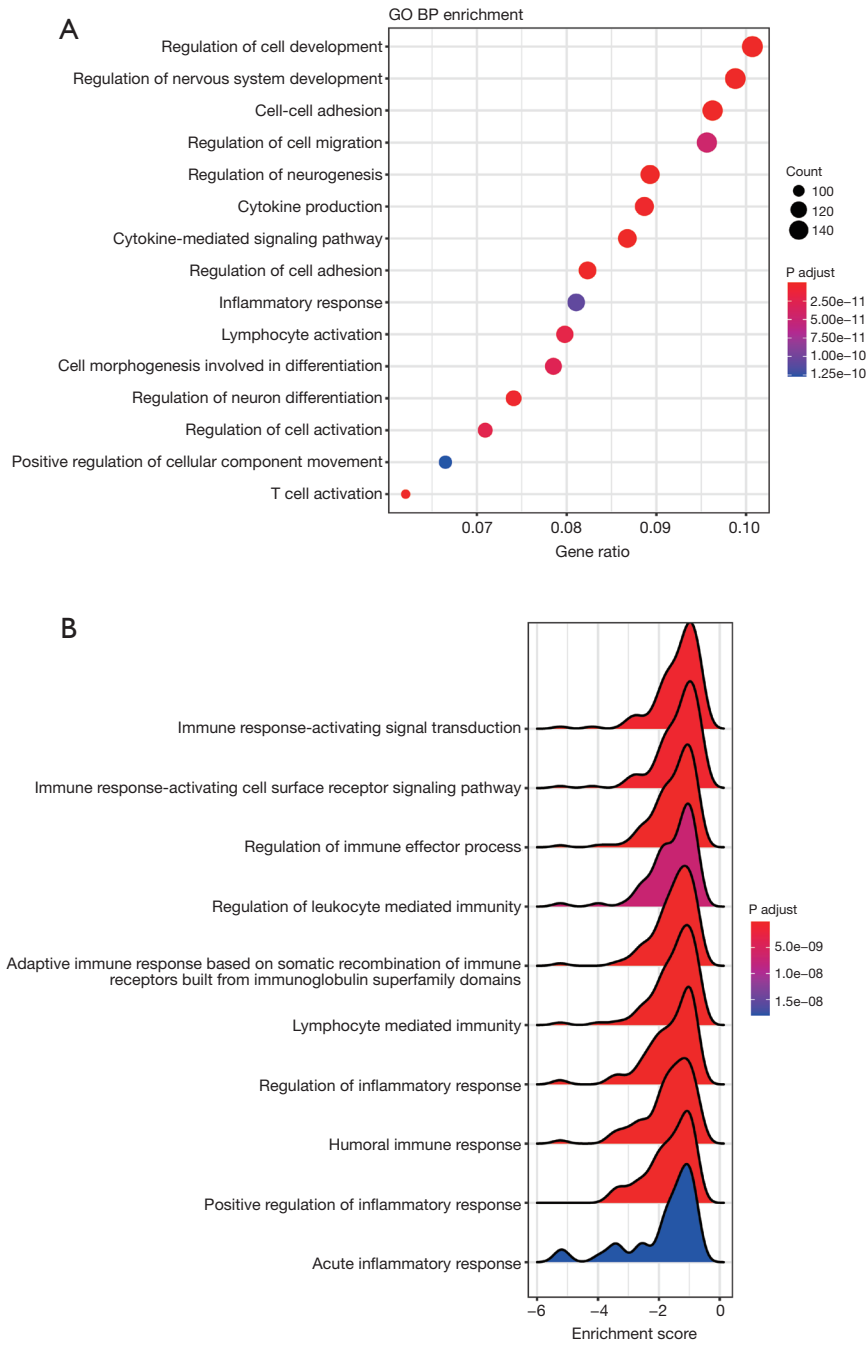


**Figure 4** The DEGs between the subtypes of *FLG* wild-type were enriched in immune-related pathways. (A) Bubble chart showing the top 15 enriched BP of DEGs. (B) Ridgeline plot showing the GSEA results. GO, Gene Ontology; BP, biological processes; DEGs, differentially expressed genes; *FLG*, filaggrin; GSEA, gene set enrichment analysis.



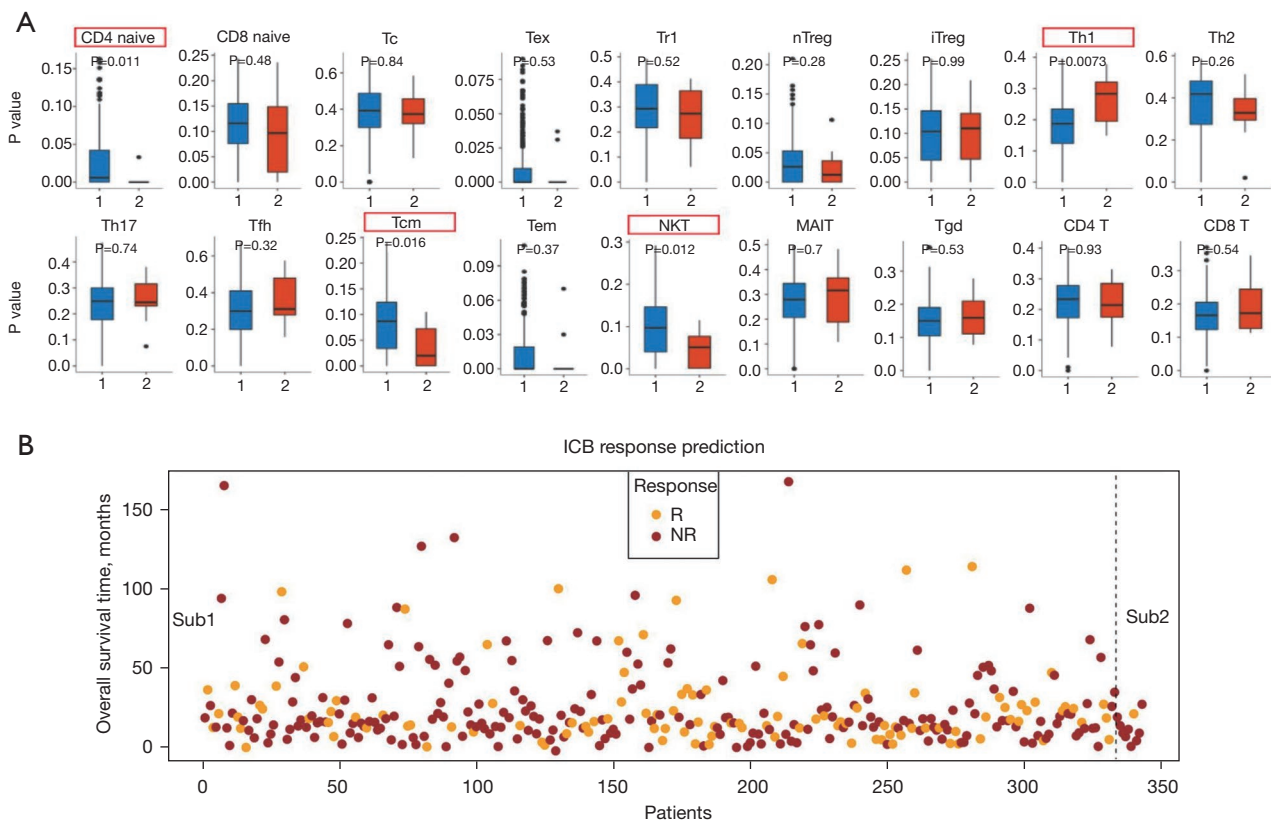


**Figure 5** Sub2 of *FLG* wild-type was associated with infiltrated immune cells and had a worse response to ICB. (A) Associations of 2 subtypes of *FLG* wild-type with infiltrated immune cells. The “1” and “2” on the abscissa represent subtype 1 and subtype 2, respectively. (B) Predicting immune checkpoints for 2 subtypes of *FLG* wild-type. ICB, immune checkpoint blockade; *FLG*, filaggrin; R, response; NR, non-response; Tc, cytotoxic T cells; Tex, exhausted T cells; Tr1, type 1 regulatory cells; nTreg, natural regulatory T cells; iTreg, induced regulatory T cells; Th1, type 1 T helper cells; Th2, type 2 T helper cells; Th17, type 17 T helper cells; Tfh, follicular helper T cells; Tcm, central memory T cells; Tem, effector memory T cells; NKT, natural killer T cells; MAIT, mucosal-associated invariant T cells; Tgd, gamma-delta T cells.

lines (Figure 6A). Hence, we chose siRNA2 for subsequent experiments. The CCK-8 assays indicated that knockdown of *FLG* could decrease the proliferation of 5637 and T24 cell lines (Figure 6B,6C). The flow cytometry experiments indicated that knockdown of *FLG* increased the apoptosis of 5637 and T24 cell lines (Figure 6D). These results revealed that *FLG* is an oncogene, and knockdown of *FLG* can suppress BLCA cell proliferation and promote apoptosis.

## Discussion

In this study, cellular experiments revealed that *FLG* is an oncogene in BLCA and knockdown of *FLG* suppressed BLCA cell proliferation and promoted apoptosis. This is the first study to show that the survival time of *FLG* wild-

type patients was significantly less than that of *FLG* mutant patients based on BLCA gene mutation data in TCGA database. Furthermore, we identified 2 different types of *FLG* wild-type patients (Sub1 and Sub2). Though the sample size of Sub2 was 10, the prognosis of Sub2 patients was worse than that of Sub1 patients, and the mortality rate of Sub2 patients was as high as 90%. Hence, we paid attention to the biological functions and pathways of Sub2 in the subsequent research. We also found that the DEGs between the subtypes of *FLG* wild-type were associated with malignant tumor proliferation and DNA damage repair. These results suggest that *FLG* wild-type subtypes play a significant role in the progression of BLCA.

Tumors are related to the accumulation of somatic mutations in cells as a result of carcinogens (24). Studies

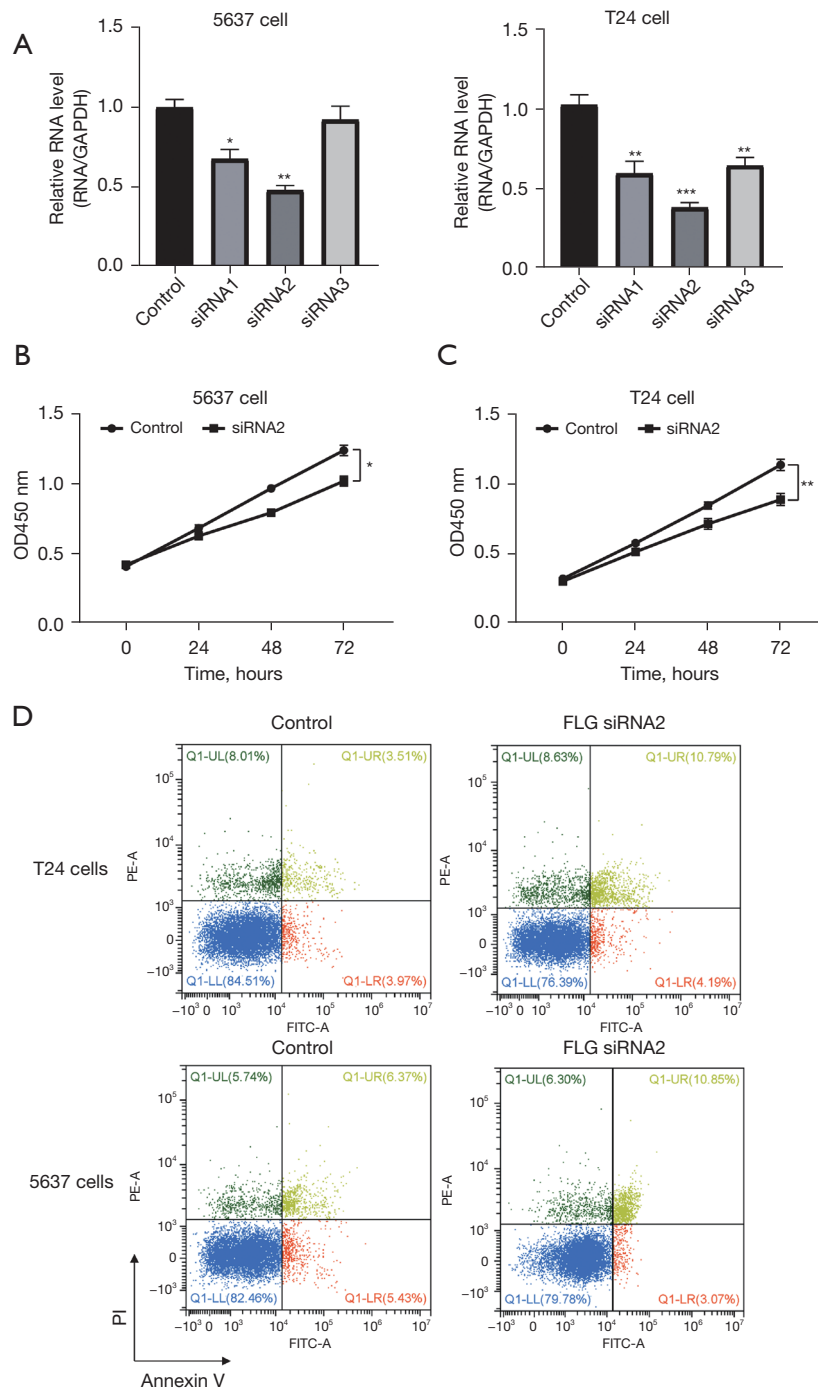


**Figure 6** Knockdown of *FLG* suppressed BLCA cell proliferation and promoted apoptosis. (A) The knockdown efficiency was detected by the qRT-PCR assay in the 5637 and T24 cell lines. (B) Analysis of cell proliferation by the CCK-8 assay was performed in the 5637 and T24 cell lines. (C,D) Analysis of cell apoptosis by flow cytometry was performed in the 5637 and T24 cell lines. \*,  $P < 0.05$ ; \*\*,  $P < 0.01$ ; \*\*\*,  $P < 0.001$ . PE-A, phycoerythrin-area; FITC-A, fluorescein isothiocyanate-area; UL, upper left quadrant; LL, lower left quadrant; UR, upper right quadrant; LR, lower right quadrant; *FLG*, filaggrin; PI, propidium iodide; BLCA, bladder urothelial carcinoma; OD, optical density.

have shown that BLCA is a highly mutated tumor type and the progression of BLCA heavily depends on the extent of gene mutation. For example, Zhang *et al.* found that BLCA patients with higher tumor mutational burden (TMB) had more survival benefits (12). In the present study, patients who had more *FLG* gene mutation also had longer survival time. The mutations of *FGFR3*, *HRAS*, *KRAS*, *NRAS*, and *PIK3CA* in BLCA are a diagnostic companion to define patients for targeted therapies (25). Recognizing genetic mutations may allow for early genetic screenings for BLCA and new therapies targeting cells with these mutations (26). Despite other potential prognostic biomarkers such as *FAGs*, *CDC20*, *EIF2S2*, *PSMA3*, *DNM1L*, *TUBA4A*, *UCHL1* and *PYCR1* have been discovered based on different criterion to classify BLCA, regardless of their mutation rates (27-30). The *FLG* gene encodes a related protein that accumulates in the intermediate filaments of mammalian epidermal keratin, and *FLG* has shown variability in the frequency variants (9). *FLG* gene mutation is one of the risk factors for cancer, as demonstrated by the associations between *FLG* loss-of-function mutations and cancer in subgroup analyses (11). Our study revealed that T cell infiltration was largely affected in patients with higher *FLG* mutation rate. In consistent with our results, previous studies have also shown that *FLG* gene mutation may exacerbate carcinogenesis, accompanied with higher tumor mutation burden and immune cell infiltration (31,32). However, the specific mechanisms remain to be explored in the future.

As one of the most common urinary system cancers worldwide, BLCA ranges from unaggressive and noninvasive tumors to aggressive and invasive tumors with high disease-specific mortality (3). However, traditional treatments have not shown significant improvements in its 5-year survival rate (33). Recently, newer immunotherapies have generated a great deal of interest in BLCA, considering that a favorable immune microenvironment should be better at fighting against the cancer evolution (34). In this study, the results of functional enrichment analysis of differential genes showed that related pathways such as inflammation, chemokine production, and T cell activation were significantly enriched. GSEA of the BP pathways suggested that the pathways related to immunity and inflammation were significantly down-regulated in Sub2, and the immune response involved in T cell activation was suppressed. Analysis of the T cell subtypes of *FLG* wild-type patients showed that Sub2 of *FLG* wild-type was correlated with infiltrating levels of immune cells ( $CD4^+$  naïve T cells,  $T_{cm}$ , and NKT cells). These results indicated that Sub2

was related to the immune microenvironment of BLCA. Investigation of the relationship and biological mechanisms between *FLG* subtypes and the immune microenvironment will help to better understand the role of immunotherapy in BLCA treatment.

Immune checkpoint inhibitors refer to inhibitory drugs developed for immune checkpoints, which can rejuvenate immune cells and kill tumor cells again (35). ICB is beneficial for restoring T lymphocyte activity and breaking through the physical barrier of the tumor immune microenvironment to promote T cell homing. The application of ICB, such as anti-programmed cell death ligand 1 (anti-PD-L1) and cytotoxic T lymphocyte-associated antigen 4 (anti-CTLA-4), is emerging as a novel treatment strategy for BLCA (36). Therefore, the prediction of immune checkpoints is of great clinical significance for BLCA. A previous study has shown a correlation between specific genetic mutations and the efficacy of immunotherapy (37). It was reported that TMB, microsatellite instability, mismatch repair gene deficiency, inflamed T cells and interferon  $\gamma$  (IFN- $\gamma$ ) gene expression profiles, and DNA damage response and antigen presentation defects may serve as potential biomarkers for immune checkpoints of immunotherapy (38). Zhang *et al.* identified *NTRK3* as a potential prognostic biomarker associated with TMB and immune infiltration in BLCA (12). Lin *et al.* found that *NCOR1* mutations may be a potential biomarker for predicting the prognosis of ICB in patients with BLCA, such as the *NCOR1*-mutant group has significantly longer overall survival than the *NCOR1*-wild-type group (39). Similarly, the application of neoadjuvant chemotherapy (NC), the standard of care for bladder cancer patients before radical cystectomy, only has promising effects in patients with certain molecular subtypes, such as the luminal-like subtypes in muscle-invasive bladder cancer (40,41). Therefore, it would be helpful to select or incorporate therapies including ICB and NC based on the gene profiles of BLCA patients. In this study, we predicted the immune checkpoints of *FLG* wild-type patients of different subtypes, and the results showed that Sub2 patients responded worse to ICB. The results suggest that this subtype of *FLG* wild-type may prove to be a novel biomarker and contribute to the development of immunotherapy for BLCA.

## Conclusions

In conclusion, this study revealed that *FLG* is an

oncogene, and knockdown of *FLG* can suppress BLCA cell proliferation and promote apoptosis. We also found that *FLG* wild-type is associated with poorer outcome in BLCA patients, and prognostic *FLG* wild-type was divided into 2 subtypes (Sub1 and Sub2). The DEGs between Sub1 and Sub2 were enriched in malignant tumor proliferation, DNA damage repair, and immune-related pathways. Furthermore, Sub2 of *FLG* wild-type was associated with infiltrated immune cells, and these patients responded worse to ICB. Accordingly, Sub2 of *FLG* wild-type may prove to be a novel diagnosis method and contribute to the development of immunotherapy for BLCA. Further experiments *in vivo* are needed for clinical validation and to investigate the underlying mechanism.

### Acknowledgments

*Funding:* None.

### Footnote

*Reporting Checklist:* The authors have completed the MDAR reporting checklist. Available at <https://tau.amegroups.com/article/view/10.21037/tau-22-573/rc>

*Data Sharing Statement:* Available at <https://tau.amegroups.com/article/view/10.21037/tau-22-573/dss>

*Conflicts of Interest:* All authors have completed the ICMJE uniform disclosure form (available at <https://tau.amegroups.com/article/view/10.21037/tau-22-573/coif>). Huina W is from Acornmed Biotechnology Co., Ltd. that has collaborative projects with Peking University People's Hospital Urology and Lithotripsy Center. The other authors have no conflicts of interest to declare.

*Ethical Statement:* The authors are accountable for all aspects of the work in ensuring that questions related to the accuracy or integrity of any part of the work are appropriately investigated and resolved. The study was conducted in accordance with the Declaration of Helsinki (as revised in 2013).

*Open Access Statement:* This is an Open Access article distributed in accordance with the Creative Commons Attribution-NonCommercial-NoDerivs 4.0 International License (CC BY-NC-ND 4.0), which permits the non-commercial replication and distribution of the article with

the strict proviso that no changes or edits are made and the original work is properly cited (including links to both the formal publication through the relevant DOI and the license). See: <https://creativecommons.org/licenses/by-nc-nd/4.0/>.

### References

1. Patel VG, Oh WK, Galsky MD. Treatment of muscle-invasive and advanced bladder cancer in 2020. *CA Cancer J Clin* 2020;70:404-23.
2. Qu G, Liu Z, Yang G, et al. Development of a prognostic index and screening of prognosis related genes based on an immunogenomic landscape analysis of bladder cancer. *Aging (Albany NY)* 2021;13:12099-112.
3. Lenis AT, Lec PM, Chamie K, et al. Bladder Cancer: A Review. *JAMA* 2020;324:1980-91.
4. Tiwari RV, Ngo NT, Lee LS. The optimal management of variant histology in muscle invasive bladder cancer. *Transl Androl Urol* 2020;9:2965-75.
5. Cao R, Ma B, Wang G, et al. Identification of autophagy-related genes signature predicts chemotherapeutic and immunotherapeutic efficiency in bladder cancer (BLCA). *J Cell Mol Med* 2021;25:5417-33.
6. Lyu Q, Lin A, Cao M, et al. Alterations in TP53 Are a Potential Biomarker of Bladder Cancer Patients Who Benefit From Immune Checkpoint Inhibition. *Cancer Control* 2020;27:1073274820976665.
7. Topalian SL, Drake CG, Pardoll DM. Immune checkpoint blockade: a common denominator approach to cancer therapy. *Cancer Cell* 2015;27:450-61.
8. Presland RB, Haydock PV, Fleckman P, et al. Characterization of the human epidermal profilaggrin gene. Genomic organization and identification of an S-100-like calcium binding domain at the amino terminus. *J Biol Chem* 1992;267:23772-81.
9. Margolis DJ, Mitra N, Wubbenhorst B, et al. Filaggrin sequencing and bioinformatics tools. *Arch Dermatol Res* 2020;312:155-8.
10. Bandier J, Ross-Hansen K, Carlsen BC, et al. Carriers of filaggrin gene (FLG) mutations avoid professional exposure to irritants in adulthood. *Contact Dermatitis* 2013;69:355-62.
11. Skaaby T, Husemoen LL, Thyssen JP, et al. Filaggrin loss-of-function mutations and incident cancer: a population-based study. *Br J Dermatol* 2014;171:1407-14.
12. Zhang Z, Yu Y, Zhang P, et al. Identification of NTRK3 as a potential prognostic biomarker associated with tumor mutation burden and immune infiltration in bladder

- cancer. *BMC Cancer* 2021;21:458.
13. Mayakonda A, Lin DC, Assenov Y, et al. Maftools: efficient and comprehensive analysis of somatic variants in cancer. *Genome Res* 2018;28:1747-56.
  14. Wu F, Chai RC, Wang Z, et al. Molecular classification of IDH-mutant glioblastomas based on gene expression profiles. *Carcinogenesis* 2019;40:853-60.
  15. Miao YR, Zhang Q, Lei Q, et al. ImmuCellAI: A Unique Method for Comprehensive T-Cell Subsets Abundance Prediction and its Application in Cancer Immunotherapy. *Adv Sci (Weinh)* 2020;7:1902880.
  16. Nordentoft I, Lamy P, Birkenkamp-Demtröder K, et al. Mutational context and diverse clonal development in early and late bladder cancer. *Cell Rep* 2014;7:1649-63.
  17. Su C, Wang X, Zhou J, et al. Titin mutation in circulatory tumor DNA is associated with efficacy to immune checkpoint blockade in advanced non-small cell lung cancer. *Transl Lung Cancer Res* 2021;10:1256-65.
  18. Xie X, Tang Y, Sheng J, et al. Titin Mutation Is Associated With Tumor Mutation Burden and Promotes Antitumor Immunity in Lung Squamous Cell Carcinoma. *Front Cell Dev Biol* 2021;9:761758.
  19. Kortylewski M, Kujawski M, Wang T, et al. Inhibiting Stat3 signaling in the hematopoietic system elicits multicomponent antitumor immunity. *Nat Med* 2005;11:1314-21.
  20. Feng H, Thasler W. Immune microenvironment modulation via the interaction of human invariant natural killer T cell (iNKT cells) and Kupffer cells (KC), dendritic cells (DC) in colorectal liver metastasis. *J Immunol* 2017;198:208.20.
  21. Borst J, Ahrends T, Bąbała N, et al. CD4+ T cell help in cancer immunology and immunotherapy. *Nat Rev Immunol* 2018;18:635-47.
  22. Mrakovcic-Sutic I, Pirjavec-Mahic A. editors. NK/NKT interactions in burn-induced changes of cell mediated immunity. 14th Congress of the International Society for Burn Injuries; Montreal, Kanada. 2008
  23. Petitprez F, Meylan M, de Reyniès A, et al. The Tumor Microenvironment in the Response to Immune Checkpoint Blockade Therapies. *Front Immunol* 2020;11:784.
  24. Dollé ME, Giese H, van Steeg H, et al. Mutation accumulation in vivo and the importance of genome stability in aging and cancer. *Results Probl Cell Differ* 2000;29:165-80.
  25. Serizawa RR, Ralfkiaer U, Steven K, et al. Integrated genetic and epigenetic analysis of bladder cancer reveals an additive diagnostic value of FGFR3 mutations and hypermethylation events. *Int J Cancer* 2011;129:78-87.
  26. Tran L, Xiao JF, Agarwal N, et al. Advances in bladder cancer biology and therapy. *Nat Rev Cancer* 2021;21:104-21.
  27. Li H, Chen S, Mi H. A Multiomics Profiling Based on Online Database Revealed Prognostic Biomarkers of BLCA. *Biomed Res Int* 2022;2022:2449449.
  28. Liu Z, Sun T, Zhang Z, et al. An 18-gene signature based on glucose metabolism and DNA methylation improves prognostic prediction for urinary bladder cancer. *Genomics* 2021;113:896-907.
  29. Luan JC, Zeng TY, Zhang QJ, et al. A novel signature constructed by ferroptosis-associated genes (FAGs) for the prediction of prognosis in bladder urothelial carcinoma (BLCA) and associated with immune infiltration. *Cancer Cell Int* 2021;21:414.
  30. Xu Y, Wu G, Li J, et al. Screening and Identification of Key Biomarkers for Bladder Cancer: A Study Based on TCGA and GEO Data. *Biomed Res Int* 2020;2020:8283401.
  31. Salerno EP, Bedognetti D, Mauldin IS, et al. Human melanomas and ovarian cancers overexpressing mechanical barrier molecule genes lack immune signatures and have increased patient mortality risk. *Oncoimmunology* 2016;5:e1240857.
  32. Zhang P, An Z, Sun C, et al. FLG gene mutation up-regulates the abnormal tumor immune response and promotes the progression of prostate cancer. *Curr Pharm Biotechnol* 2022. [Epub ahead of print]. doi: 10.2174/1389201023666220413092507.
  33. Cheng W, Fu D, Xu F, et al. Unwrapping the genomic characteristics of urothelial bladder cancer and successes with immune checkpoint blockade therapy. *Oncogenesis* 2018;7:2.
  34. Vasekar M, Degraff D, Joshi M. Immunotherapy in Bladder Cancer. *Curr Mol Pharmacol* 2016;9:242-51.
  35. Day D, Hansen AR. Immune-Related Adverse Events Associated with Immune Checkpoint Inhibitors. *BioDrugs* 2016;30:571-84.
  36. Mukherji D, Jabbour MN, Saroufim M, et al. Programmed Death-Ligand 1 Expression in Muscle-Invasive Bladder Cancer Cystectomy Specimens and Lymph Node Metastasis: A Reliable Treatment Selection Biomarker? *Clin Genitourin Cancer* 2016;14:183-7.
  37. Wang F, Zhao Q, Wang YN, et al. Evaluation of POLE and POLD1 Mutations as Biomarkers for Immunotherapy Outcomes Across Multiple Cancer Types. *JAMA Oncol* 2019;5:1504-6.

38. Wang S, He Z, Wang X, et al. Antigen presentation and tumor immunogenicity in cancer immunotherapy response prediction. *Elife* 2019;8:49020.
39. Lin A, Qiu Z, Zhang J, et al. Effect of NCOR1 Mutations on Immune Microenvironment and Efficacy of Immune Checkpoint Inhibitors in Patient with Bladder Cancer. *Front Immunol* 2021;12:630773.
40. Buttigliero C, Tucci M, Vignani F, et al. Molecular biomarkers to predict response to neoadjuvant chemotherapy for bladder cancer. *Cancer Treat Rev* 2017;54:1-9.
41. Sjö Dahl G, Abrahamsson J, Holmsten K, et al. Different Responses to Neoadjuvant Chemotherapy in Urothelial Carcinoma Molecular Subtypes. *Eur Urol* 2022;81:523-32.

**Cite this article as:** Chen L, Huang X, Xiong L, Chen W, An L, Wang H, Hong Y, Wang H. Analysis of prognostic oncogene filaggrin (*FLG*) wild-type subtype and its implications for immune checkpoint blockade therapy in bladder urothelial carcinoma. *Transl Androl Urol* 2022;11(10):1419-1432. doi: 10.21037/tau-22-573

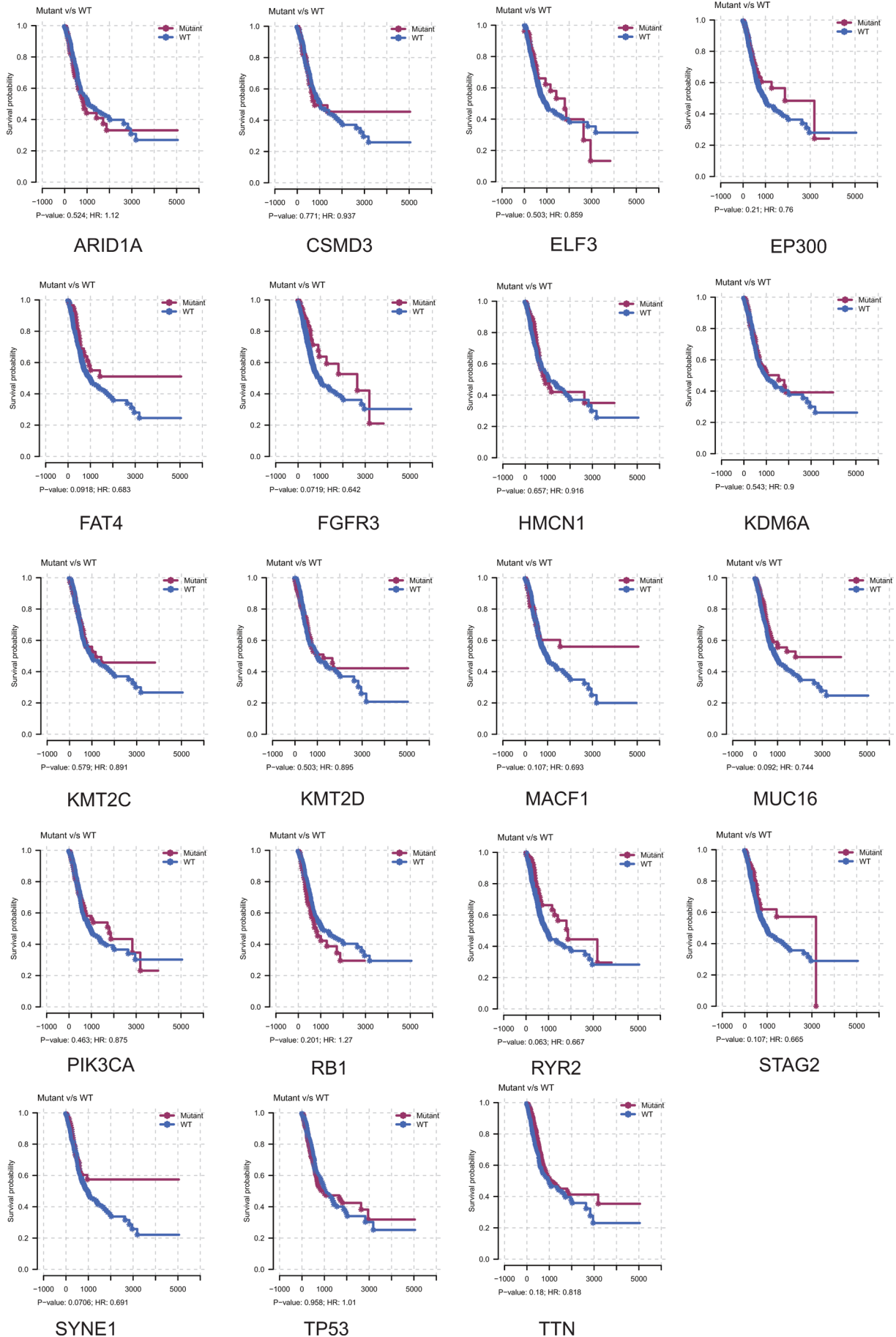


**Figure S1** The prognostic analysis of the top 19 mutant genes. v/s, versus; WT, wild type; HR, hazard ratio.

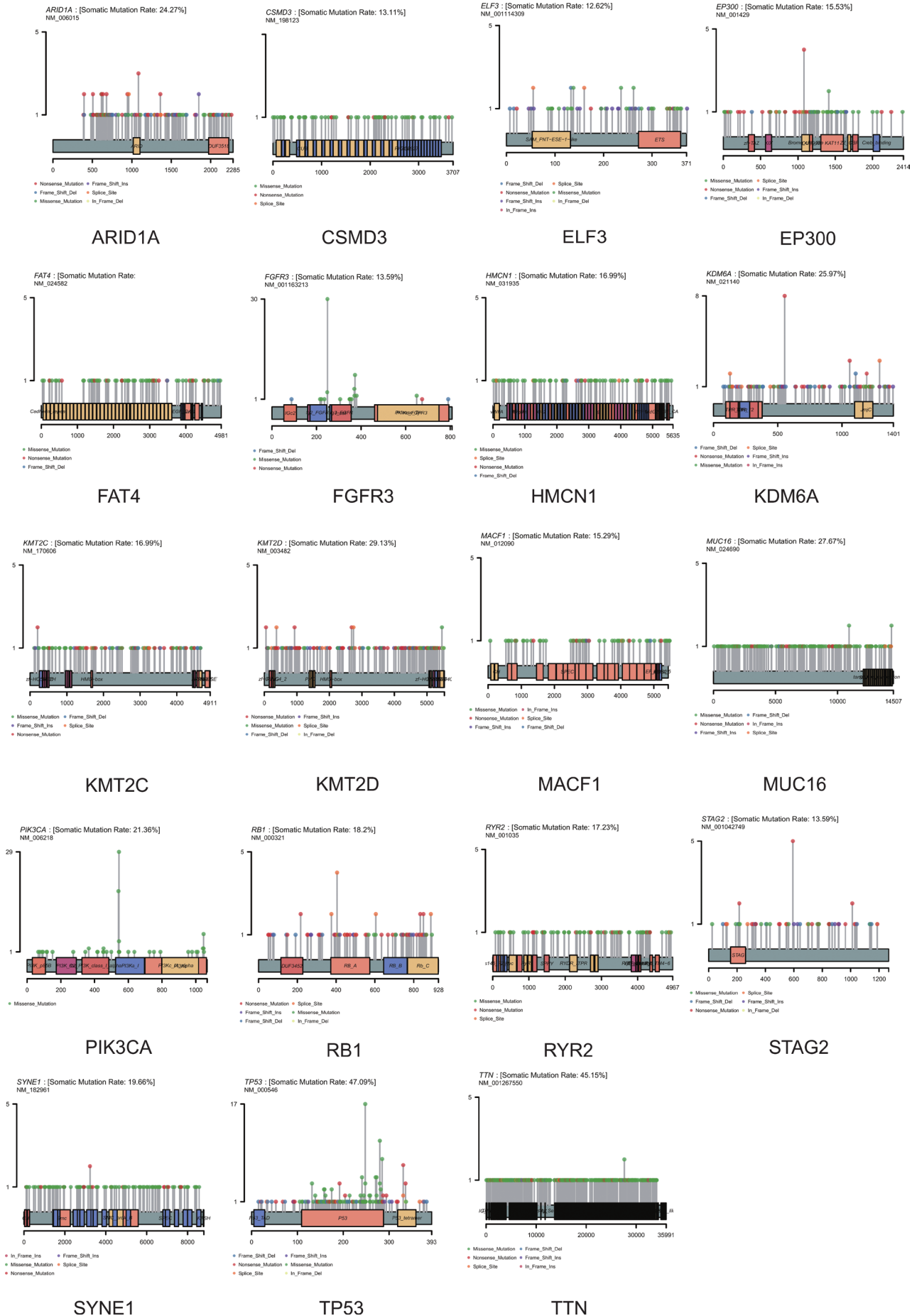


**Figure S2** The mutation forms of other top 19 mutant genes. v/s, versus; WT, wild type; HR, hazard ratio.